Electronic Supplementary Information

Two-dimensional heterotriangulene-based manganese organic frameworks: bipolar magnetic and half semiconductors with perpendicular magnetocrystalline anisotropy

Yue Wang, Jiawei Jiang, Wenbo Mi*

Tianjin Key Laboratory of Low Dimensional Materials Physics and Preparation Technology, School of Science, Tianjin University, Tianjin 300354, China

*Author to whom all correspondence should be addressed.
E-mail: miwenbo@tju.edu.cn

A. Computational Methods of nearest-neighbor exchange integral and anisotropy constant

The $q = \sqrt{3} \times \sqrt{3}$ frustrated AFM state was calculated based on the *XYZ* Heisenberg Hamiltonian which is defined as

$$H = -\sum_{\langle i,j \rangle} J(S_i^x S_j^x + S_i^y S_j^y + k_u S_i^z S_j^z)$$

Where k_u is the anisotropy constant, $0 \le k_u \le 1$. It becomes the *XY* model and isotropic Heisenberg model when k_u=0 and 1, respectively.[1] The nearest-neighbor exchange integral J_1 can be obtained through the formula:

$$J_1 = (E_{\mathrm{AFM}} - E_{\mathrm{FIM}}) / (2|S|^2)$$

The magnetic anisotropy energy E_{MAE} can be expressed as

$$E_{\mathrm{MAE}} = 8J|k_u - 1||S|^2$$

The calculated results show that k_u is in the range of 0.3 to 0.7. According to the ground-state phase diagram deduced in a previous theoretical study,[2] the ground state of the *X*TPA-Mn and *X*TPB-Mn (*X*=M, C and O) with S=5/2 and 0.3<k_u<0.7 is q=0 frustrated antiferromagnetic order.

Table S1 Lattice constant a (Å) of unit cell OTPA-Mn, energy difference $\Delta E_{FM\text{-}AFM}$ and $\Delta E_{FIM\text{-}AFM}$ (eV), magnetic moment M_{Mn} (μ_B) of Mn atom and total magnetic moment M_{FM} and M_{FIM} (μ_B) adopted with different effective U_{eff} (eV).

U_{eff}	0	1	2	3	4
a	21.65	21.68	21.73	21.74	21.81
$\Delta E_{FM\text{-}AFM}$	44.93	28.66	17.67	8.6	7.41
$\Delta E_{FIM\text{-}AFM}$	7.19	5.2	3.82	3.6	2.55
M_{Mn}	4.31	4.40	4.48	4.53	4.60
M_{FM}	15.00	15.00	15.00	15.00	15.00
M_{FIM}	5.00	5.00	5.00	5.00	5.00

Table S2 Lattice constant (a) and band gap (E_g) of XTPA and XTPB (X=M, C and O).

	MTPA	CTPA	OTPA	MTPB	CTPB	OTPB
a (Å)	17.45	17.37	17.10	17.64	17.61	17.20
E_g (eV)	1.67	1.74	1.09	2.14	1.30	2.07

Table S3 Calculated structure of *X*TPA-Mn and *X*TPB-Mn (*X*=M, C and O)

	MTPA-Mn	CTPA-Mn	OTPA-Mn	MTPB-Mn	CTPB-Mn	OTPB-Mn
d_1 (Å)	2.07	2.04	2.07	2.06	2.08	2.07
d_2 (Å)	1.42	1.41	1.39	1.52	1.52	1.47
d_3 (Å)		1.24	1.40		1.24	1.40
d_4 (Å)	1.10	1.09	1.09	1.10	1.09	1.09
θ_1 (°)	120.00	120.00	119.88	119.95	120.00	119.90
θ_2 (°)	120.00	120.00	120.01	119.98	120.00	120.00
M_C (μ_B)	-0.06	-0.06	-0.06	-0.06	-0.06	-0.06

Mn-C bond length (d_1), N/B-C bond length (d_2), O-C bond length (d_3), C-H bond length (d_4) Mn-Mn-Mn bond angle (θ_1), C-N/B-C (θ_2), magnetic moments of adjacent C atoms (M_C)

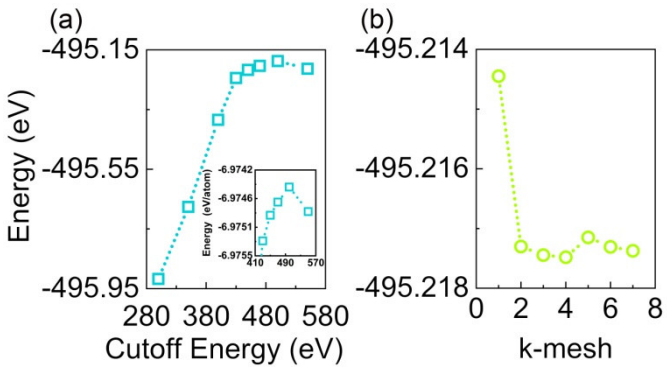

Fig. S1 Test of (a) cutoff energy and (b) *k*-mesh for MTPB-Mn. The inset of (a) is the energy per atom around convergent cutoff energy.

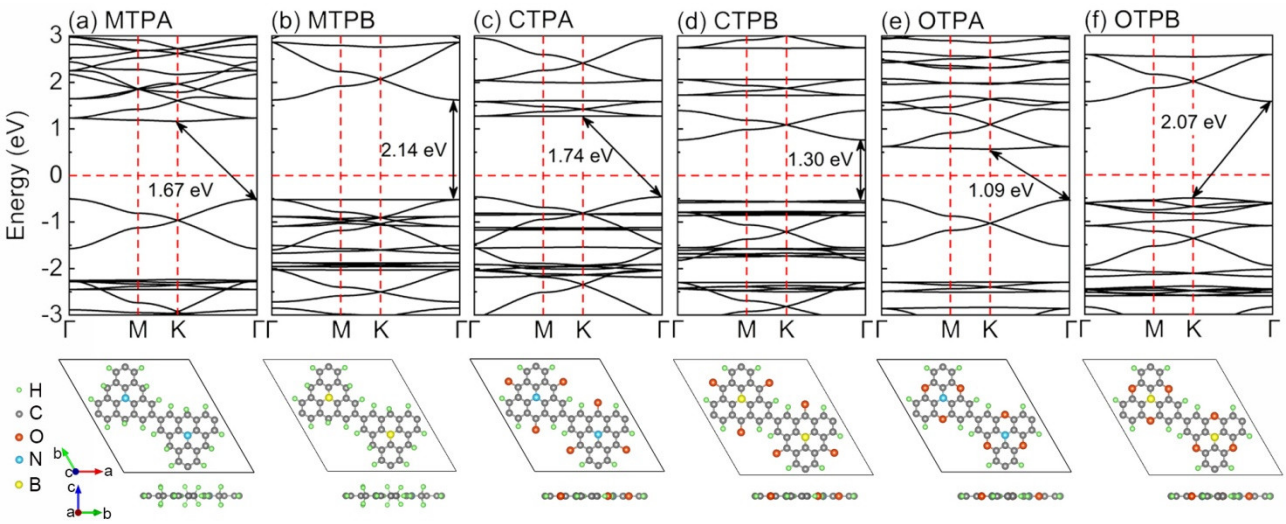

Fig. S2 The band and lattice structures of (a) MTPA, (b) MTPB, (c) CTPA, (d) CTPB, (e) OTPA and (f) OTPB, respectively.

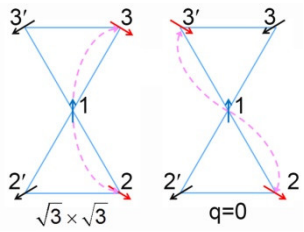

Fig. S3 $\sqrt{3} \times \sqrt{3}$ and q=0 spin configurations.

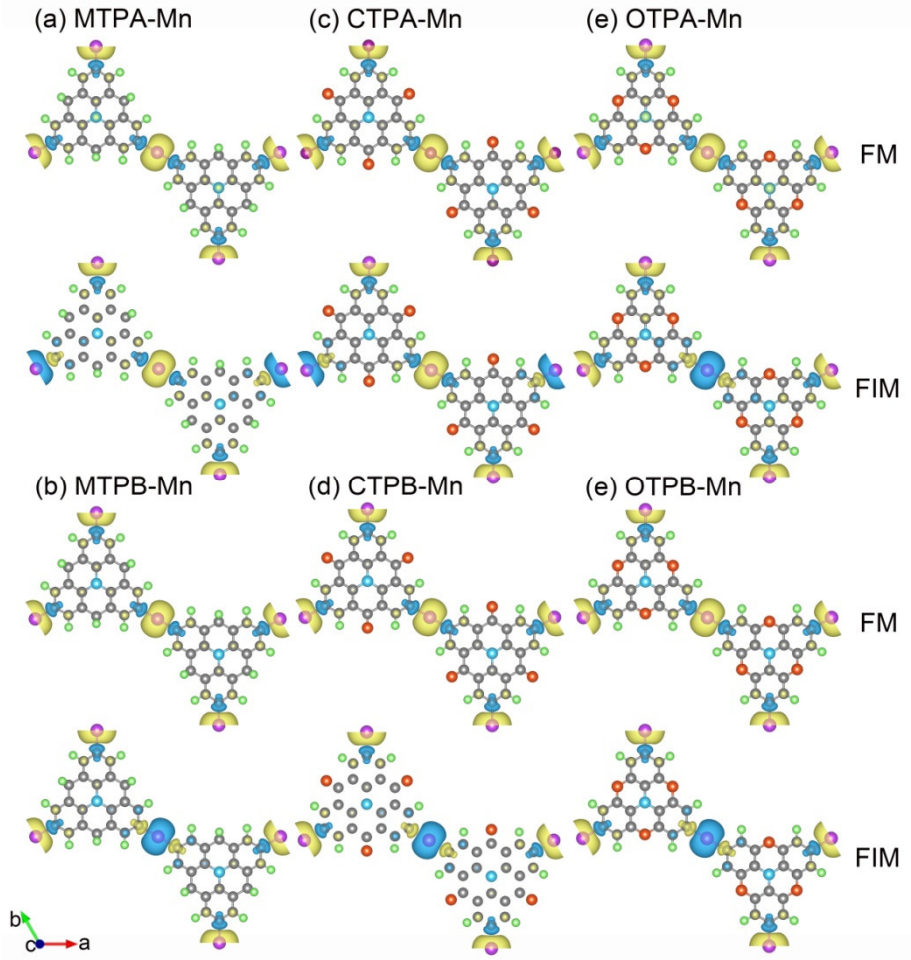

Fig. S4 Top views of spin-polarized electron density for (a) MTPA-Mn, (b) MTPB-Mn, (c) CTPA-Mn, (d) CTPB-Mn, (e) OTPA-Mn and (f) OTPB-Mn in FM and FIM states, respectively. The isosurface value is 0.002 e/Bohr^3. Yellow and blue regions represent the positive and negative values, respectively.

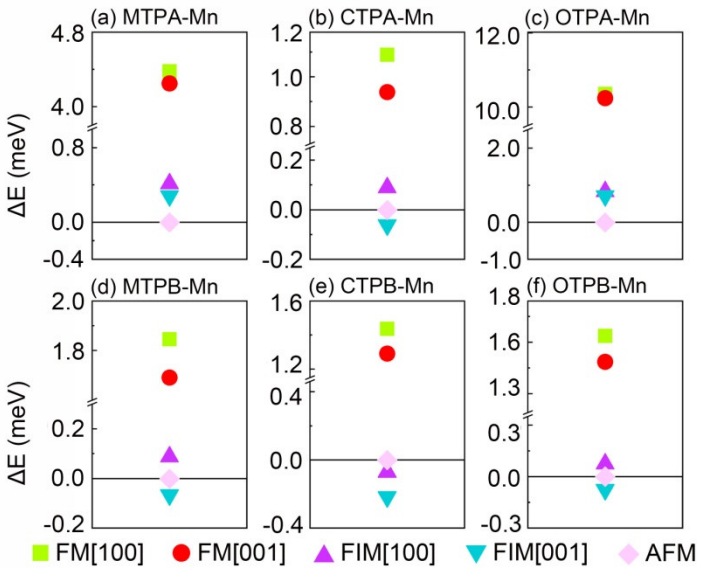

Fig. S5 The energy difference of (a) MTPA-Mn, (b) CTPA-Mn, (c) OTPA-Mn, (d) MTPB-Mn, (e) CTPB-Mn and (f) OTPB-Mn with SOC, respectively. The energy of AFM is set to zero.

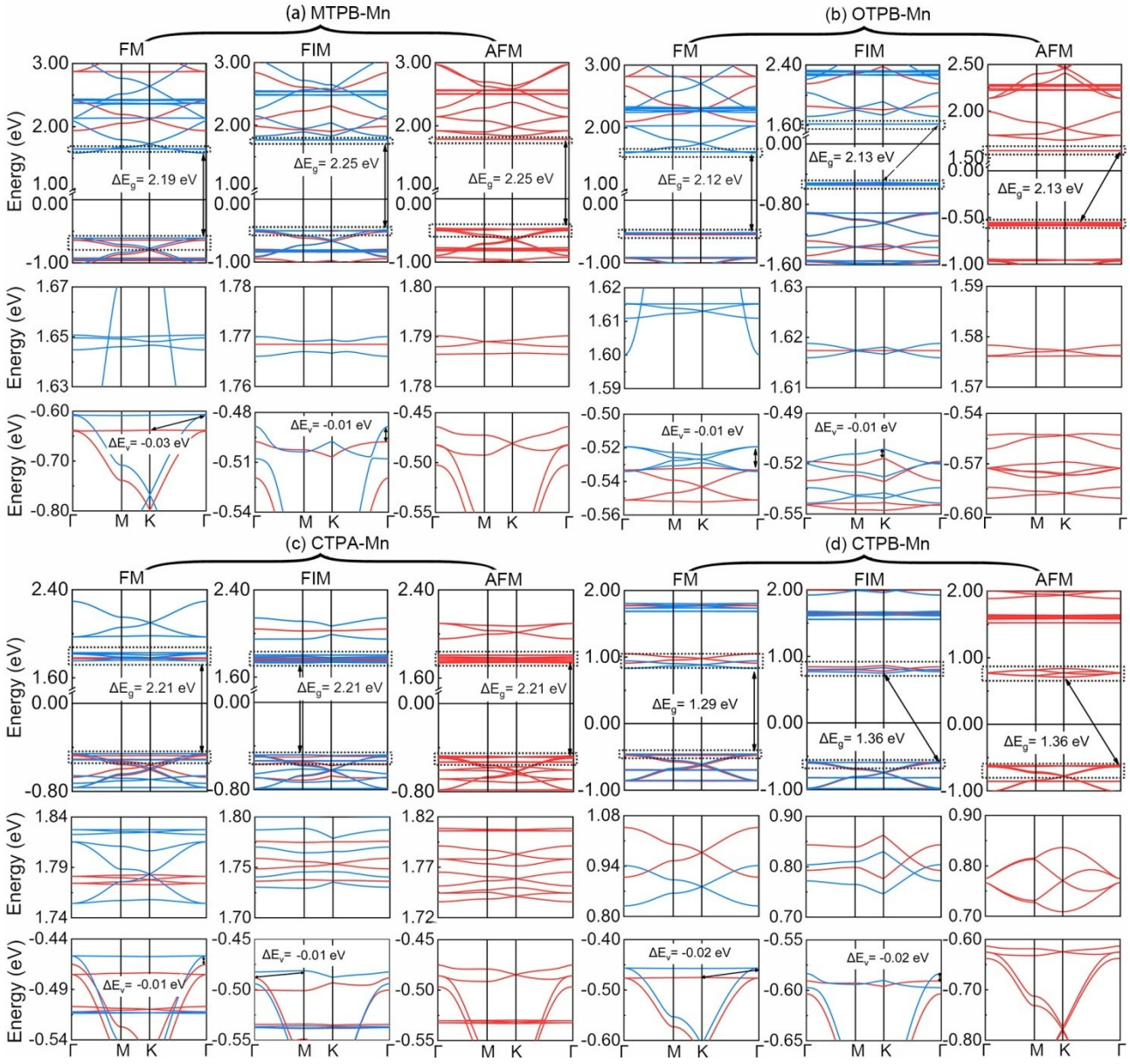

Fig. S6 The band structures around Fermi level, CB and VB for (a) MTPA-Mn, (b) OTPB-Mn, (c) CTPA-Mn and (d) CTPB-Mn in FM, FIM and AFM configurations, respectively. The Fermi level is set to zero. The red (blue) lines represent the spin-up (spin-down) channel.

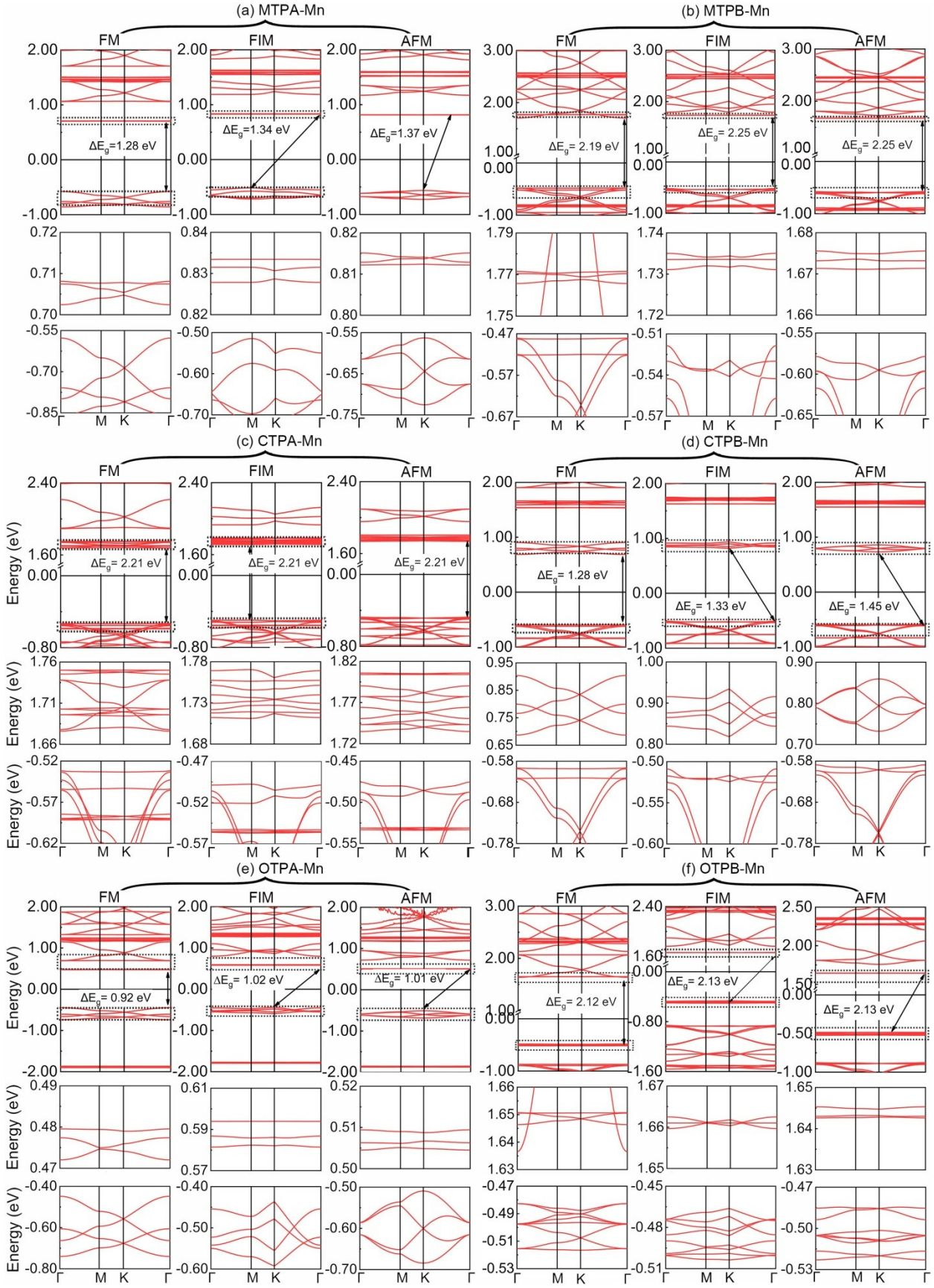

Fig. S7 The band structures around Fermi level, CB and VB for *X*TPA-Mn and *X*TPB-Mn (*X*=M, C and O) with SOC.

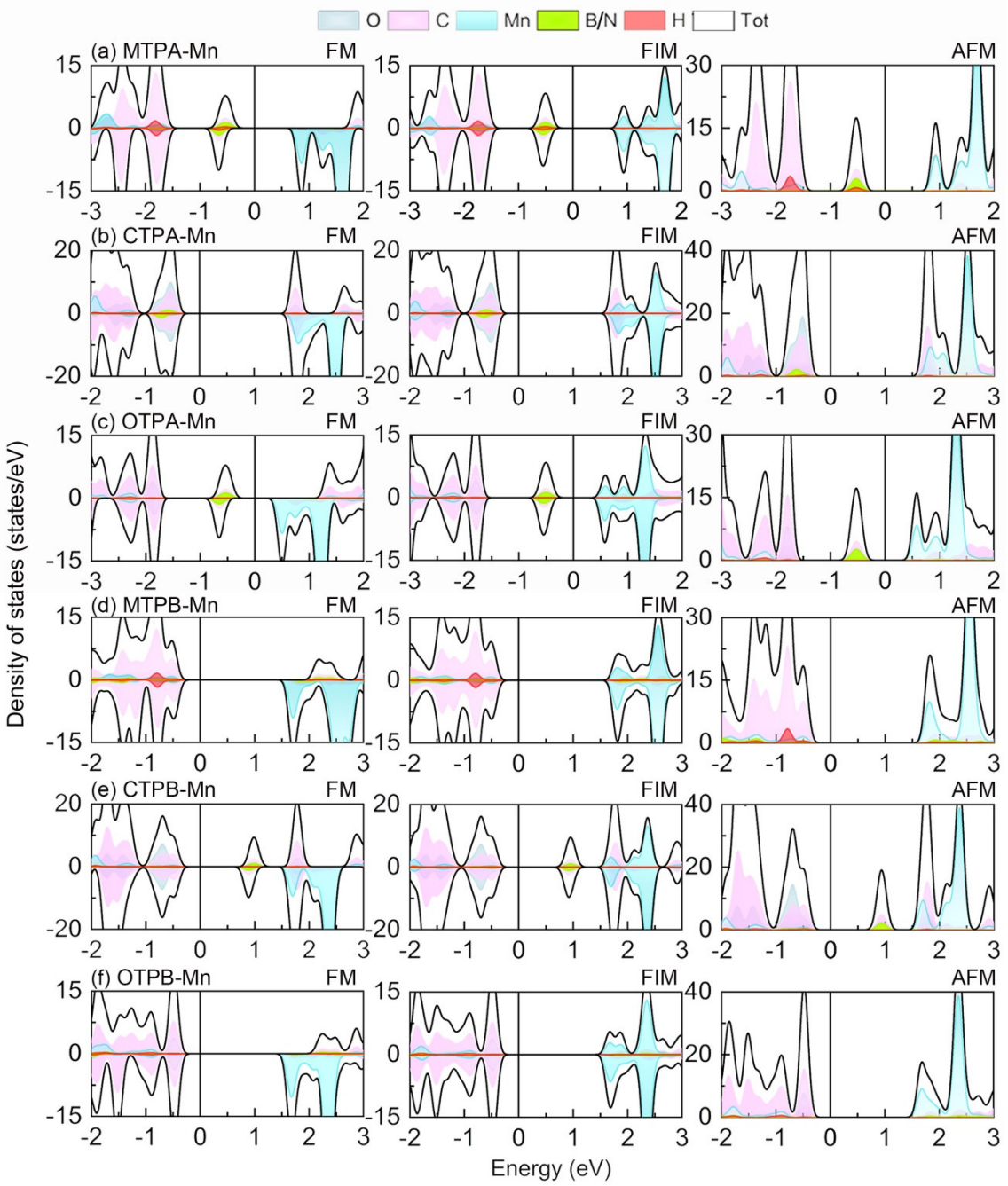

Fig. S8 The local and total DOS of (a) MTPA-Mn, (b) CTPA-Mn, (c) OTPA-Mn, (d) MTPB-Mn, (e) CTPB-Mn and (f) OTPB-Mn in FM, FIM, AFM configurations, respectively. The positive and negative values represent the spin-up and spin-down channel, respectively.

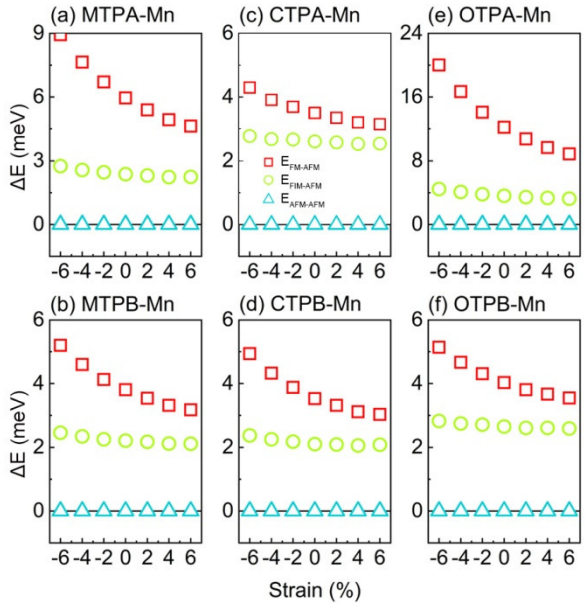

Fig. S9 The energy difference ΔE of (a) MTPA-Mn, (b) CTPA-Mn, (c) OTPA-Mn, (d) MTPB-Mn, (e) CTPB-Mn and (f) OTPB-Mn, respectively. FM, FIM with respect to the AFM under different biaxial strain. The energy of AFM is set to zero.

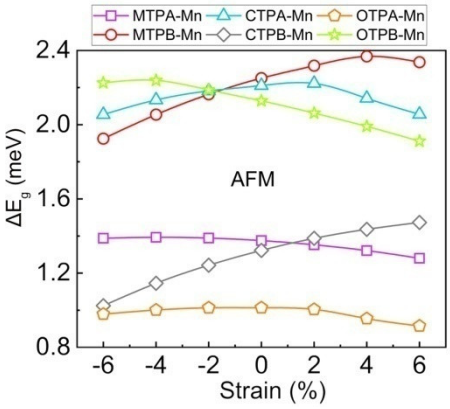

Fig. S10 Strain-dependent band gap ΔE_g of *X*TPA-Mn and *X*TPB-Mn (*X*=M, C and O) in AFM state.

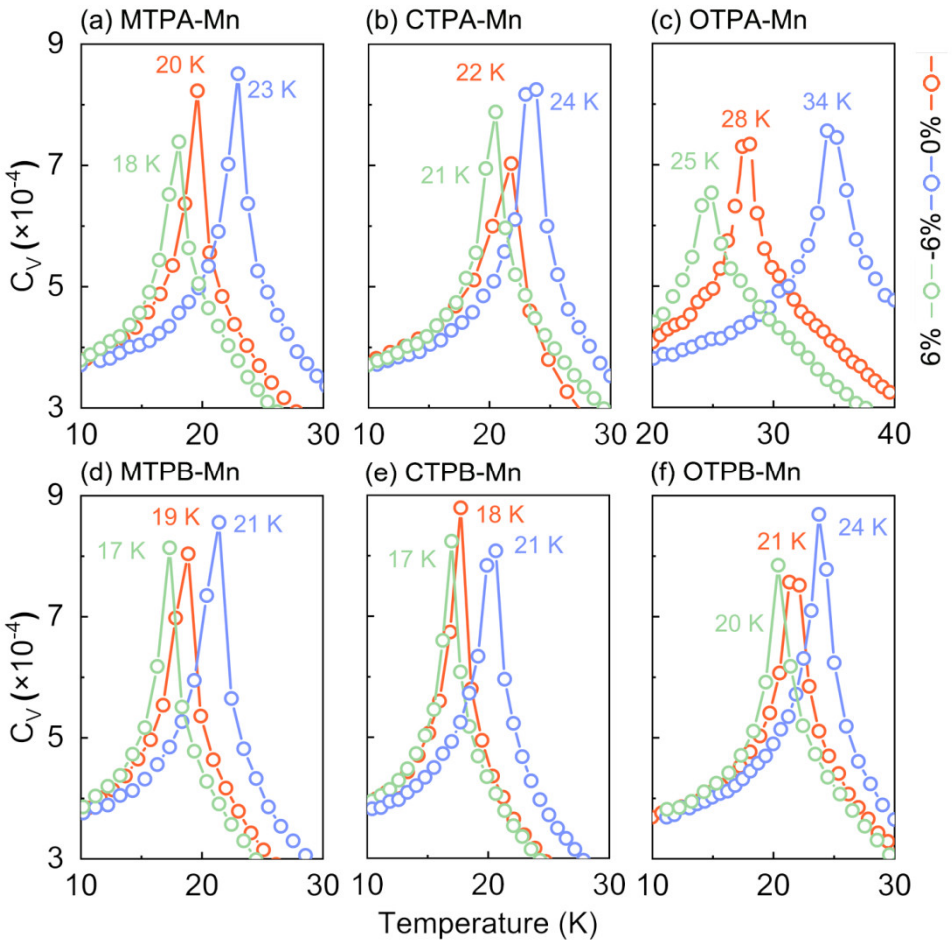

Fig. S11 Evolution of the Monte Carlo averaged specific heat capacity for *X*TPA-Mn and *X*TPB-Mn (*X*=M, C and O) as a functional of temperature.

References

1 P. Müller, A. Zander and J. Richter, Phys. Rev. B 2018, 98, 024414.

2 O. Götze and J. Richter, Phys. Rev. B 2015, 91, 104402.